

LASPA: Latent Spatial Alignment for Fast Training-free Single Image Editing

Yazeed Alharbi¹ and Peter Wonka²

¹ NCAI
² KAUST

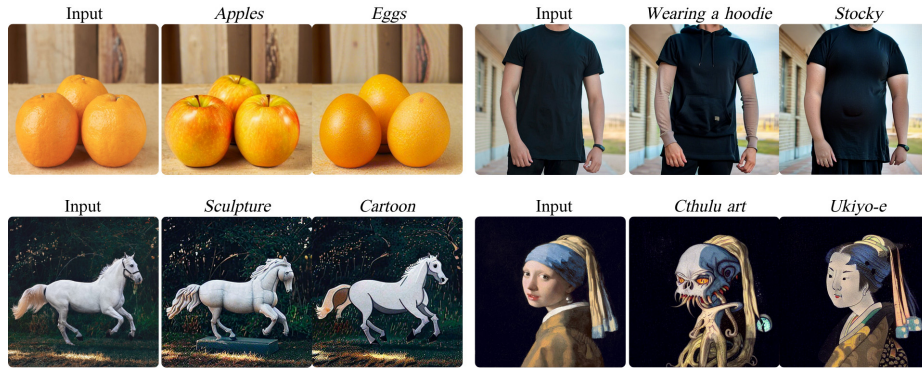


Fig. 1: Using a single real image as input, our method is capable of editing using textual prompts in less than 6 seconds without finetuning the diffusion model or using costly image embedding algorithms. Our results show accurate editing for realistic as well as artistic edits.

Abstract. We present a novel, training-free approach for textual editing of real images using diffusion models. Unlike prior methods that rely on computationally expensive finetuning, our approach leverages LATent SPatial Alignment (LASPA) to efficiently preserve image details. We demonstrate how the diffusion process is amenable to spatial guidance using a reference image, leading to semantically coherent edits. This eliminates the need for complex optimization and costly model finetuning, resulting in significantly faster editing compared to previous methods. Additionally, our method avoids the storage requirements associated with large finetuned models. These advantages make our approach particularly well-suited for editing on mobile devices and applications demanding rapid response times. While simple and fast, our method achieves 62-71% preference in a user-study and significantly better model-based editing strength and image preservation scores.

Keywords: Text-to-image · Diffusion model · Fast Editing

1 Introduction

Text-to-image diffusion models [2, 3, 8, 27–29, 31] have revolutionized image generation, creating realistic and diverse images from textual prompts. However,

harnessing these models for single-image editing remains a challenge, as it requires preserving the original image details while generating the required edits. Traditionally, editing with generative models involves inverting the input image into the latent space of the generator to preserve details, and then manipulating the latent to achieve the desired edit. Diffusion models offer advantages for both inversion and editing due to their spatial latents. The latents carry rich spatial information and can be easily reproduced given real images using the noise schedule.

Despite the potential of the spatial latents, state-of-the-art single-image editing methods [16, 21, 39] rely on textual tokens while finetuning the model’s parameters to encode reference image information. This forgoes the advantages of spatial latents, leading to longer processing times and increased storage needs. While the last two years have brought fantastic improvements in diffusion-based image editing, the computational cost and memory overhead of these methods are significant. Existing work [10, 16, 21, 30, 39] is confined to editing speeds in the order of minutes while requiring the storage of a separate finetuned model per image or edit. However, image-editing applications require results almost instantly, as users on mobile devices, desktop applications, or cloud-based services, are only willing to wait for a few seconds to achieve an edit. Further, cloud-based services require cheap computation costs to be profitable, and mobile devices require simple and memory-efficient computation in general.

To address these limitations, we do not propose acceleration strategies of existing methods, but an alternative method on how edits can be achieved that is conceptually much simpler. We present LASPA, a novel approach for single-image editing using text-to-image diffusion models. We propose leveraging real image information to guide the spatial latents, while keeping the textual latents intact. By eliminating the need for optimization and finetuning, LASPA addresses the computational constraints that may otherwise limit the widespread adoption of diffusion-based image editing.

Specifically, in lieu of optimizing or finetuning to preserve the input image, we align any random latent using reference image features directly using different parts of the reverse diffusion process. Our knowledge of the amount of noise added to training samples at each timestep enables aligning the input sample x_t . Our knowledge of the denoising UNet allows aligning the predicted error ϵ_θ . Our knowledge of a good initial estimate for x_0 enables alignment of the prediction of x_0 .

We perform qualitative and quantitative experiments to validate the gains of our method. We show that our method is consistently preferred by users, and leads to better image preservation and editing strength model-based scores.

2 Related work

Diffusion models for image generation: Diffusion models [7, 13, 14, 23, 28, 32, 34, 40] offer excellent results for image synthesis. A unique aspect of diffusion models is that they operate on images or spatial latents extracted by pretrained

VQ models [9]. This is a major deviation from previous generative models, GANs, where vectors were used as latents.

For editing with unconditional diffusion models DiffusionCLIP [17] shows interesting results. Given a diffusion model trained on a specific class (for example, faces), the authors show how the CLIP loss can be used to perform textual edits. Crucially, DiffusionCLIP shows that image reconstruction is noticeably more accurate with diffusion models than GANs. FreeDoM [36] proposes training-free conditional editing for unconditional models, such that images or text can be used.

Recent diffusion models [2, 3, 8, 24, 25, 27–29] offer prompt-based control over the generated images. They allow almost unlimited control over the generated images such as generating in a certain artist’s style or generating fictional creatures. This is achieved through cross-attention between a spatial image latent and a textual latent. Given the amount of training data and the quality of results, a new area of research aspired to leverage the learned text-image associations for other tasks.

Controllable generation with text-to-image diffusion models: One of the earlier works for controlling images generated by diffusion models is prompt-to-prompt [12]. Prompt-to-prompt shows that attention maps learned by stable diffusion are useful to preserve the semantic layout of generated images. However, prompt-to-prompt fails to preserve the identities of objects. Therefore it requires specialized embedding algorithms, such as Null-text inversion [21] to edit real images. One strand of work is to train separate auxiliary networks to inject conditioning information, such as segmentation or depth maps. Currently, ControlNet [37] and Lora [15] are very popular for this task.

Real image editing with text-to-image diffusion models: Several works in the literature propose editing improvements such as better inversion methods [22, 33], better scoring functions [11], and improvements to editing with stochastic models [35]. More recently, there are two emerging research problems: model personalization and single image editing.

Model personalization aims to capture a concept using a few images such that the text-to-image model can regenerate it in novel views and edit it. While single image editing uses text-to-image models to enable text-based editing of real images given only a single image. Most previous methods for single image editing or model personalization [10, 16, 30, 39] utilize the textual embedding to encode the identity of objects to be preserved. As a result, previous methods require either finetuning the entire model or optimizing the textual token. These methods require minutes to edit while requiring the storage of a finetuned model per edit or image.

While some prior methods enable faster editing [1, 4, 6, 20], they are very limited in comparison with methods that require finetuning. SDEdit [20] often fails to preserve identity information, while blended diffusion [1] and DiffEdit [6] are restricted to local edits. InstructPix2Pix [4] offers inference time editing using textual instructions and shows convincing results. However, it requires training a model with a large generated set of text and image pairs.

3 Method

3.1 Motivation

To motivate our approach, we review diffusion model training and inference. Diffusion models are trained by adding noise to training images according to a predefined schedule. This is referred to as the diffusion process. The noised training sample x_t is a linear combination of original image information x_0 and added noise $\epsilon \sim \mathcal{N}(0, Id)$ according to predetermined weights α :

$$x^t = \sqrt{\alpha_t}x_0 + \sqrt{1 - \alpha_t}\epsilon \quad (1)$$

A crucial observation is that the reference image in editing tasks can be easily diffused to any timestep. This can be done by adding noise according to the training schedule.

The transformer UNet is trained to predict the noise/error at any timestep through the following loss function:

$$\mathcal{L}(\epsilon_\theta) = \|\epsilon_\theta^{(t)}(\sqrt{\alpha_t}x_0 + \sqrt{1 - \alpha_t}\epsilon_t) - \epsilon_t\|_2^2 \quad (2)$$

Another important observation is that we can also easily compute the reconstruction error at any timestep of the reverse diffusion process. This can be done by computing the difference between the reference image and the partially denoised sample at the current timestep.

We use DDIM sampling [32], where the error $\epsilon_\theta^{(t)}$ predicted by the transformer UNet is used to predict the final result x_0 from the current result x_t :

$$pred_{x_0}^{(t)} = \frac{x_t - \sqrt{1 - \alpha_t}\epsilon_\theta^{(t)}(x_t)}{\sqrt{\alpha_t}} \quad (3)$$

This prediction of x_0 is used to compute the next denoised estimation x_{t-1} given the current x_t :

$$x_{t-1} = \sqrt{\alpha_{t-1}}pred_{x_0}^{(t)} + \sqrt{1 - \alpha_{t-1}}\epsilon_\theta^{(t)}(x_t) \quad (4)$$

Where the right-hand term of the addition is referred to as the direction pointing to x_t . We observe that for the task of editing, an initial prediction of x_0 can be easily obtained directly using the reference image.

Our observations about the generative reverse diffusion process form the basis of our methodology. We claim that several components of the generative reverse diffusion process are receptive to spatial guidance using reference image features directly.

3.2 Latent spatial alignment

Given a reference image I and a prompt P , the goal of prompt-based image editing is to produce an image \hat{I} that remains as similar as possible to I while reflecting the edits specific by P .

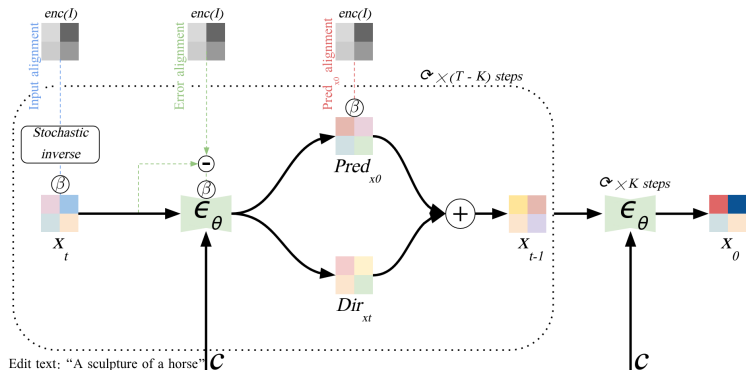


Fig. 2: An illustration of our alignment methods and how they influence reverse diffusion steps.

There are two types of latents in text-to-image diffusion models: spatial latents and textual latents. The spatial latents are noised visual information being either images I or latents $enc(I)$ extracted using a pre-trained autoencoder (e.g. the $64 \times 64 \times 4$ tensor that is gradually transformed in Stable Diffusion [29]). The textual latents are extracted from P and are used to condition the generation results. Contrary to the common approach of encoding the image into textual latents, we propose latent spatial alignment to edit using reference image features directly, without requiring optimization or changing the model’s parameters.

LASPA demonstrates how different components of the reverse diffusion process are receptive to latent spatial alignment. The key insight is that we can align the network using real image information to produce a reverse diffusion path that starts by aiming to reconstruct I while slowly introducing the edits highlighted in P .

All of our proposed alignment paths follow this intuition. They are training-free, they align only the spatial latents, and they lead to *exact* reconstruction of $enc(I)$ if the reconstruction path is followed for all reverse diffusion steps. However, they differ significantly in how they guide reconstruction and how they can be used to guide editing. One reason for our achieved speedup is that the proposed alignment strategies eliminate the need for image inversion as we can initialize with arbitrary noise x_T .

3.3 Input alignment

The most direct way to encourage the preservation of input image features is to inject the reference features into a certain timestep. This is possible because we have access to the exact training schedule used to introduce noise at each timestep of diffusion. However, directly injecting a noised version of the input image at a certain timestep is problematic. Injecting early allows for editing, but fails to preserve details of the image. This is the approach used in SDEdit [20].



Fig. 3: Our latent alignment smoothly incorporates information from both the editing prompt and the input image. The editing prompt used is "a photo of an angry woman."

Injecting later preserves almost all the details of the input image but heavily restricts editing.

Instead of a one-step injection, we propose aligning the spatial latent with the input at each timestep using reference image features. We start with an unrestricted random noise input, and we slowly align it to the stochastic inversion at the start of each timestep. The stochastic inverse is a weighted combination of a sampled random noise $z \sim \mathcal{N}(0, Id)$ and the encoded input image $enc(I)$. This leverages the stochastic inversion to preserve spatial details of the input image while allowing P freedom for editing.

$$z \sim \mathcal{N}(0, Id), \quad \beta_t = \frac{t}{T}, \quad K \in [0, T] \quad (5)$$

$$x_t^{stochinv} = \sqrt{\alpha_t} \times enc(I) + \sqrt{1 - \alpha_t} \times z \quad (6)$$

$$\hat{x}_t = \begin{cases} \beta_t \times x_t^{stochinv} + (1 - \beta_t) \times x_t, & t > K \\ x_t & t \leq K \end{cases} \quad (7)$$

Where β controls the alignment strength, K controls the alignment interval, and α_t is a scheduling weight that follows the training procedure.

As shown in Figure 3, we find that the aligned latent begins by encoding large-scale features of the reference image, while reflecting the textual edit. For example, aligning until $t = 700$ aligns the pose and color information, aligning until $t = 400$ adds the eyeglasses and hairstyle, and aligning until 100 adds most identity information.

There are two interesting aspects about input alignment. First, it aligns using the stochastic inverse. Second, input alignment directly aligns the input x_t to the UNet at each timestep, which can overwrite edits in previous steps that contradict image information. As a result, it leads to high image preservation and low editing strength.

3.4 ϵ_θ alignment

Instead of directly aligning the input, possibly overwriting some editing details, we can indirectly align samples by aligning the output of the UNet ϵ_θ . While

the UNet is trained for unconditional and conditional denoising, we can align it to preserve the input image. Given the latent of the input image $enc(I)$, we can compute the actual error between x_t and $enc(I)$ exactly. We use this to align the denoising error to the reconstruction error. This follows the same intuition of input alignment: the aligned latent should first move towards recreating $enc(I)$, then slowly move towards reflecting P .

$$\hat{\epsilon}_\theta(x_t) = \begin{cases} \beta_t \times (x_t - enc(I)) + (1 - \beta_t) \times \epsilon_\theta(x_t), & t > K \\ \epsilon_\theta(x_t) & t \leq K \end{cases} \quad (8)$$

Input alignment and error alignment can work with DDPM or DDIM samplers. However, there are important differences. First, error alignment uses the difference with the current sample to align. As a result, it is more dependent on previous steps. Second, in DDIM samplers, error alignment affects both terms of the update: prediction of x_0 and direction of x_t . This is illustrated in Figure 2 and Equation 4. The computed error ϵ_t is *subtracted* to obtain the prediction of x_0 , and then *added* to obtain x_{t-1} . Consequently, error alignment is more difficult to tune and leads to higher editing strength at the cost of lower image preservation.

3.5 Prediction of x_0 alignment

Finally, we propose a more intuitive alignment that follows our reasoning of aligning between the reconstruction path and the editing path. Since DDIM [32] samplers use the error $\epsilon_\theta(x_t)$ to predict the denoising result x_0 at every step, we can align this prediction using reference image features directly. The intuition is that in early steps the prediction should be close to $enc(I)$, while in later steps the prediction should be allowed more freedom to introduce P .

$$\hat{pred}_{x_0}^{(t)} = \begin{cases} \beta_t \times enc(I) + (1 - \beta_t) \times pred_{x_0}^{(t)}, & t > K \\ pred_{x_0}^{(t)} & t \leq K \end{cases} \quad (9)$$

By simply aligning the prediction of x_0 , any random input can be aligned to reflect both image details while reflecting the textual edit. In comparison with input and error alignment, this alignment method uses the reference image encoding directly to align. Furthermore, this method imposes the least restrictions as it only aligns a part of the DDIM update. As a result, it provides the best tradeoff between editing strength and image preservation, and we use it for all evaluation results in the paper.

3.6 Real image understanding

Our approach aims to leverage spatial information of real images without fine-tuning. This raises the concern of whether our method simply pastes real image information over images conditioned on P leading to artifacts or contradicting information. To address this concern, we examine the attention maps produced

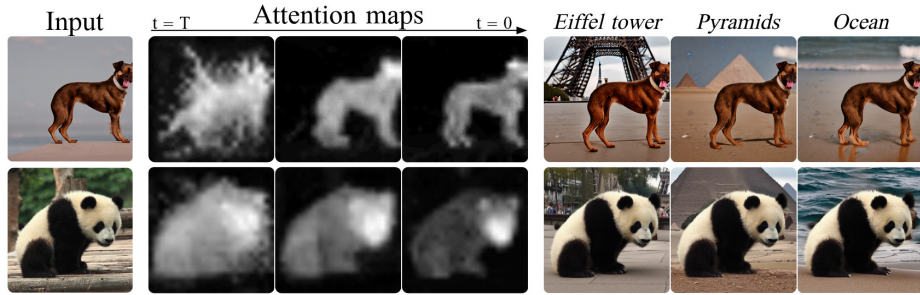


Fig. 4: Our proposed alignment methods lead to accurate attention maps and can be used for background editing using semantic latent mixing.

by the UNet during inference. We run our method with prompts that contain the coarse class of the object in the image. For example, “an image of a *panda*”. Then, we visualize the attention maps of the coarse class word.

As seen in Figure 4, we find that our proposed alignment leads to accurate attentions maps for real images. The impact is that our alignment for editing leads to accurate training-free attention maps. In comparison, methods for editing real images based on prompt-to-prompt typically require minutes of optimization to produce attention maps.

3.7 Semantic latent mixing

To further demonstrate the semantic coherence of our method, we leverage the accurate attention maps obtained through alignment to improve editing results in certain cases. In cases where large background changes are needed, we synthesize the final image such that information pertaining to the coarse class will be influenced by the aligned latent, thus maintaining the identity. On the other hand, information pertaining to the rest of the prompt will be influenced by a latent conditioned on P .

In essence, we use the attention maps of the coarse object class as an editing mask for alignment. Thus, the semantic latent mixing updated would be:

$$\hat{x}_t^{(t)} = \begin{cases} x_t^{aligned} \bullet M + x_t \bullet (1 - M), & t > K \\ x_t & t \leq K \end{cases} \quad (10)$$

We observe in Figure 4 that the final result of editing is semantically coherent, such that information is exchanged between I and the editing details. This is accomplished through both the self-attention and the cross-attention of the diffusion model. Self-attention, by design, allows each region within the mixed latent to be affected by other regions. We also adjust the cross-attention mechanism to further improve the coherence of the final image. We swap the attention maps of the mixed latent with the attention maps of the aligned latent, similar to prompt-to-prompt. This improves cases where the reverse diffusion process

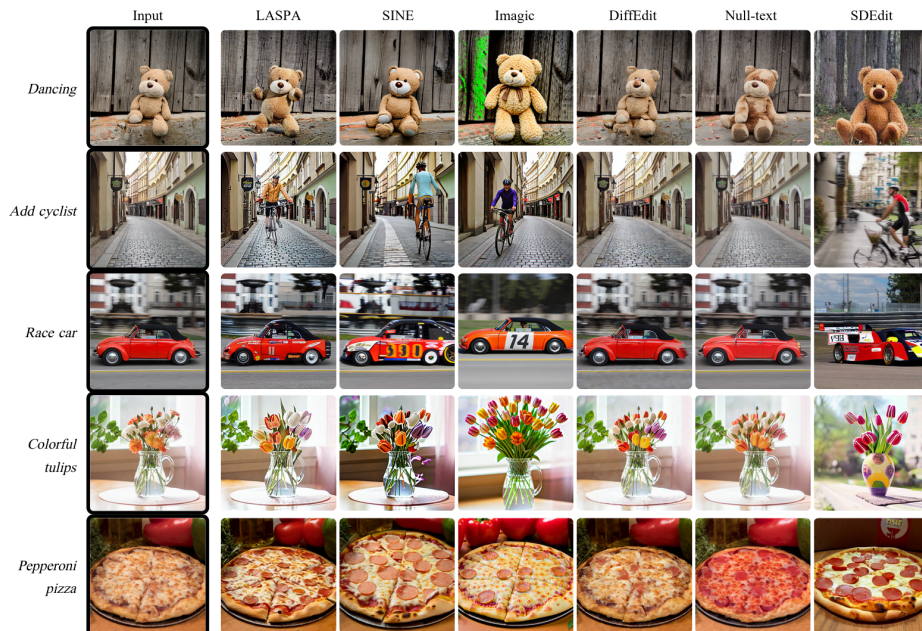


Fig. 5: A visual comparison of editing results between state-of-the-art methods and our method (LASPA). Our method exceeds the quality of methods that require finetuning, while editing only at inference time.

adds another object of the same class in a different location.

We use semantic latent mixing to showcase the semantic coherence of our method in Figures 4 and 6. However, for all other results, we use latent alignment without semantic mixing.

4 Evaluation

4.1 Implementation details

For all our qualitative and quantitative experiments, we use stable-diffusion 1.4 with 512×512 resolution. However, in the supplementary material, we show additional results on stable-diffusion 2.1 with resolution 768×768 . For most visual and tabular results in this paper, we choose $K = 200$, $\beta = 0.3$, the stable-diffusion prompt scale to be 10, the number of steps to be 50, and we use $pred_{x_0}$ alignment. Similar to Asyrp [18], we find that breaking the symmetry by using a different ϵ_θ improves editing results.

4.2 Qualitative comparison

In all explored examples, it is evident that our utilization of the spatial latent to encode image details, rather than textual tokens, leads to higher quality of edit-



Fig. 6: While null-text inversion requires minutes for inversion, LASPA aligns the spatial latent at inference time while producing less noisy attention maps.

ing. We compare against SINE [39], Imagic [16], and Null-text inversion [21]. Additionally, we include results against faster textual editing methods: DiffEdit [6] and SDEdit [20]. The results can be seen in Figure 5. Against methods that require training (Imagic, SINE, and Null-text inversion) our method leads to much better preservation of input image details while still reflecting the required edits. Against faster methods (SDEdit and DiffEdit) our method is more advantageous in all aspects. DiffEdit and Null-text inversion are more suitable for object replacements and do not introduce most required edits. SDEdit reflects the edits but strays far from input image details. Our method, while being as fast as SDEdit and DiffEdit leads to higher quality editing than methods that require finetuning such as SINE and Imagic.

To highlight the semantic coherence of our method, we compare the quality of extract attention maps for different objects. As seen in Figure 6, our method leads to less noisy attention maps when compared to Null-text inversion. Null-text inversion requires minutes of optimization to invert the input image. In comparison, our method extracts the attention maps relating to the object keyword during inference-time alignment. The accuracy of the attention maps suggests that reference image features are used to guide the semantics of the final generated image.

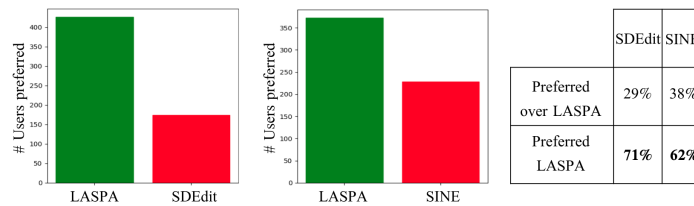


Fig. 7: Our method is preferred by users to the inference-time method SDEdit over 70% of the time. In comparison to SINE, which requires finetuning, our method is preferred over 60% of the time.

	CLIP-T \uparrow	LPIPS \downarrow	Time	Additional Storage
<i>Default</i>				
Imagic	0.3035	0.5925	8 (m)	8GB per edit
SINE	0.3035	0.5120	15 (m)	8GB per image
SDEdit	0.3031	0.5630	6 (s)	0GB
Ours	0.3042	0.4579	6 (s)	0GB
<i>Config A</i>				
SINE	0.3000	0.4110	15 (m)	8GB per image
SDEdit	0.2969	0.5560	6 (s)	0GB
Ours	0.3001	0.3337	6 (s)	0GB
<i>Config B</i>				
SINE	0.2973	0.2817	15 (m)	8GB per image
SDEdit	0.2870	0.3094	6 (s)	0GB
Ours	0.2978	0.2501	6 (s)	0GB

Table 1: A comparison of image preservation and edit strength similarity scores as measured by CLIP text-image similarity and LPIPS on the TEdBench dataset. Our method leads to the highest editing strength while being the most similar to the input image. Configs A and B explore different preservation-editing tradeoffs.

4.3 Quantitative comparison

We perform two sets of experiments to validate our gains. First, we conduct a user study and ask users to select the editing result they prefer. Second, similar to previous works, we use model-based similarity metrics such as LPIPS [38], and CLIP text similarity [26].

For the user study, we compare against SDEdit, which offers inference-time editing, and SINE, which requires finetuning. We collect over 1200 responses on different images and edits. As shown in Figure 7, our method is preferred significantly more often than SDEdit and SINE. While our method is inference-time, it is still preferable by users to SINE which requires over 15 minutes of finetuning per image.

We also make use of the TEdBench dataset [16], which contains 100 edits on many images. We compare against Imagic, SINE, and SDEdit. As shown in Table 1, our method significantly reduces perceptual distance without harming editing strength. For LASPA, SINE, and SDEdit, we produce multiple results with different tradeoffs to showcase how our method leads to better results.

4.4 Time and memory consumption

We compare the time and memory consumption of our method against SINE, SDEdit, and Imagic in Table 1.

SINE requires over 15 minutes given the reference image to finetune the network for future edits. Imagic requires around 8 minutes of finetuning for each edit. Our method, on the other hand, can handle any edit in less than 6 seconds. In terms of memory, SINE requires storing a finetuned model per input image, and

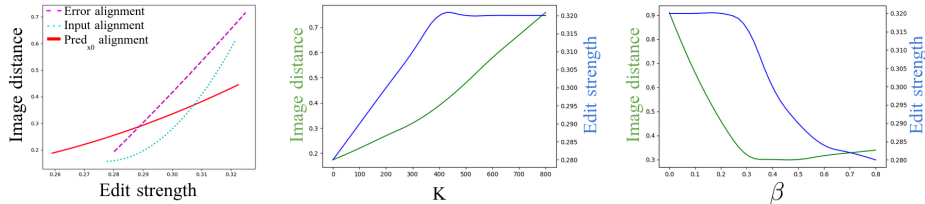


Fig. 8: Left: A comparison of the preservation-editing tradeoff between the different alignment methods. Middle and right: plots showing how image preservation and editing strength are affected by parameter choice.

requires using the outputs of two different networks at inference time. Imagic requires storing a finetuned model and a textual embedding for each pair of reference image and edit prompt. In comparison, our method does not require additional storage or running different models at inference time. We use the same pre-trained stable-diffusion model for all input images and all edit prompts. While SDEdit is fast and requires storing only a single stable-diffusion model, it leads to significantly worse results both in terms of input preservation and editing strength.

4.5 Ablation studies

To perform the ablation studies, we compute the LPIPS image distance and CLIP text similarity metrics on a smaller subset of images and editing prompts. The analysis is shown in Figure 8.

First, we analyze the behavior of the various alignment methods in the left subplot of the figure. Input alignment leads to the highest image preservation if alignment is performed in all steps. This is because it directly aligns the input samples, possibly disregarding edits performed in earlier steps. However, for more drastic edits, when the alignment interval and strength are reduced, input alignment struggles with input preservation. We hypothesize that this is due to the usage of the stochastic inverse which is dominated by noise in early steps. This results in lower preservation if alignment is terminated early.

Prediction of x_0 leads to the best tradeoff between image preservation and editing strength, especially when larger edits are needed. This is due to how it only aligns one branch of the DDIM update. It uses the input image features directly, and it can generate acceptable results with as low as 20 steps.

Error alignment is the most difficult to tune, as the error appears in opposite signs in the DDIM update. We find that it requires a higher β than other methods to preserve the input image details.

Additionally, We evaluate the influence of two main parameters: the alignment interval K , and the alignment strength β to understand their influence on the final performance. As shown in the middle and right subplots in Figure 8, our method works reasonably well on a wide range of parameter choices. The tradeoff between image preservation and editing strength can be controlled

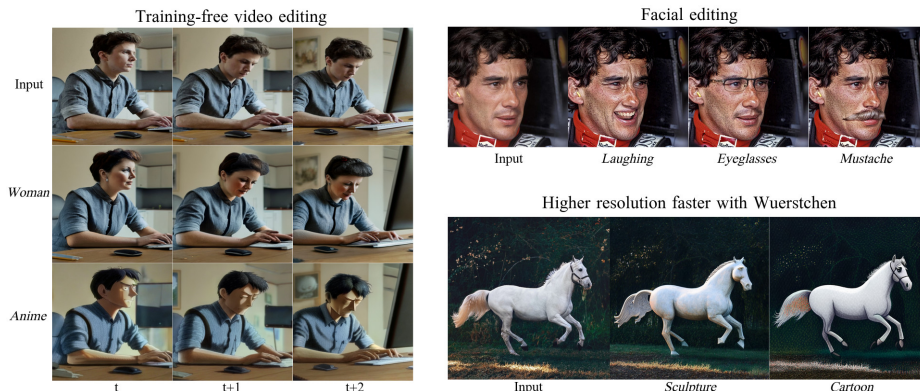


Fig. 9: LASPA shows promise for future work in video editing, facial editing, and efficient editing.

through the parameter choices. Intuitively, running our method with a longer alignment interval (lower K), and higher alignment strength (higher β) leads to higher image preservation at the cost of editing strength.

4.6 Discussion

The qualitative and quantitative analysis consistently show that our method leads to better image preservation than prior methods while still improving faithfulness to editing prompts. The results support our claim that the spatial latent is more suitable for encoding image details than the textual latent.

SINE and Imagic finetune stable-diffusion parameters based on a single image. Consequently, some of their editing results show artifacts or saturated colors leading to lower quality and lower image preservation. In addition, they necessitate storing a separate finetuned model per image or per edit, which is not scalable as shown in Table 1. SDEdit and DiffEdit do not require finetuning, but they are more suitable for specific edits. SDEdit performs poorly when extended to textual edits, and is more suitable for conditioning using segmentation maps. DiffEdit excels at localized and object replacement edits. However, it struggles with artistic, global, and object addition edits.

In contrast, our approach aligns entirely within the pretrained spatial and textual latents of text-to-image diffusion models. This leads to several essential benefits. Our method is significantly faster and significantly more similar to the input image, while surpassing the editing strength of previous methods. Furthermore, our method can handle both local and global kinds of edits

5 Future work and Limitations

We find that spatial latent alignment is versatile and shows promise for future work in video editing, facial editing, and more efficient image editing. This is

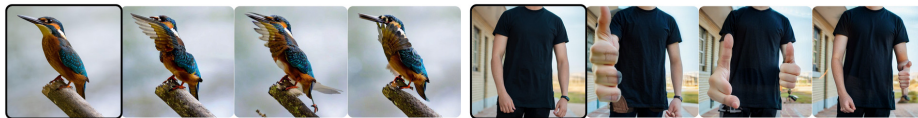


Fig. 10: Example failure cases of our method. Input images are outlined. The edits are: spreading wings, and giving a thumbs up. Three random results are generated for each input image.

illustrated in Figure 9. We find that when applied to frames of a video, our method achieves frame consistency without temporal information. With stricter alignment, our method leads to high-quality facial editing results. We note that the writing on the clothing is unchanged by our method. Finally, our method is not restricted to stable diffusion. We use Wuerstchen [24] to showcase 1024×1024 resolution results in only 3 seconds.

In terms of limitations, similar to other image editing methods, we find that the results can be improved by tuning parameters based on the kind of editing and by selecting better seeds. Another limitation is the difficulty of achieving some large pose changes. We show some failure cases of this kind in Figure 10. Evidently, some kinds of edits are more difficult to achieve given only a single image and require tools such as MasaCtrl [5].

6 Conclusion

This paper introduces LASPA, a novel framework for single-image editing using pre-trained text-to-image diffusion models. LASPA achieves significant improvements in both editing speed and quality, consistently generating edits in under 6 seconds while surpassing the quality of previous methods. This efficiency stems from LASPA’s utilization of the spatial latent for editing, eliminating the need for computationally expensive fine-tuning or storing separate models for each edit.

LASPA offers three distinct approaches to latent spatial alignment for effectively preserving input image details throughout the editing process. These approaches involve aligning the input at each step, aligning the predicted initial latent state, or directly aligning the denoising error. Additionally, LASPA demonstrates the semantic value of its aligned latents by utilizing the pre-trained model’s attention maps to achieve accurate background modifications.

LASPA’s key strengths lie in its exceptional speed, minimal computational requirements, and competitive editing quality. This paves the way for the development of user-friendly and customizable image editing applications, particularly in scenarios where traditional approaches are impractical due to their computational demands. We believe LASPA represents a significant step forward in diffusion-based image editing, offering a powerful tool for both researchers and developers seeking to create fast, high-quality, and accessible editing experiences.

References

1. Avrahami, O., Lischinski, D., Fried, O.: Blended diffusion for text-driven editing of natural images. In: Proceedings of the IEEE/CVF Conference on Computer Vision and Pattern Recognition. pp. 18208–18218 (2022)
2. Balaji, Y., Nah, S., Huang, X., Vahdat, A., Song, J., Zhang, Q., Kreis, K., Aittala, M., Aila, T., Laine, S., Catanzaro, B., Karras, T., Liu, M.Y.: ediff-i: Text-to-image diffusion models with ensemble of expert denoisers. arXiv preprint arXiv:2211.01324 (2022)
3. Betker, J., Goh, G., Jing, L., Brooks, T., Wang, J., Li, L., Ouyang, L., Zhuang, J., Lee, J., Guo, Y., et al.: Improving image generation with better captions. Computer Science. <https://cdn.openai.com/papers/dall-e-3.pdf> **2**(3), 8 (2023)
4. Brooks, T., Holynski, A., Efros, A.A.: Instructpix2pix: Learning to follow image editing instructions. In: Proceedings of the IEEE/CVF Conference on Computer Vision and Pattern Recognition. pp. 18392–18402 (2023)
5. Cao, M., Wang, X., Qi, Z., Shan, Y., Qie, X., Zheng, Y.: Masactrl: Tuning-free mutual self-attention control for consistent image synthesis and editing (2023)
6. Couairon, G., Verbeek, J., Schwenk, H., Cord, M.: Diffedit: Diffusion-based semantic image editing with mask guidance (2022)
7. Dhariwal, P., Nichol, A.: Diffusion models beat gans on image synthesis. Advances in neural information processing systems **34**, 8780–8794 (2021)
8. Ding, M., Yang, Z., Hong, W., Zheng, W., Zhou, C., Yin, D., Lin, J., Zou, X., Shao, Z., Yang, H., et al.: Cogview: Mastering text-to-image generation via transformers. Advances in Neural Information Processing Systems **34**, 19822–19835 (2021)
9. Esser, P., Rombach, R., Ommer, B.: Taming transformers for high-resolution image synthesis. In: Proceedings of the IEEE/CVF conference on computer vision and pattern recognition. pp. 12873–12883 (2021)
10. Gal, R., Alaluf, Y., Atzmon, Y., Patashnik, O., Bermano, A.H., Chechik, G., Cohen-Or, D.: An image is worth one word: Personalizing text-to-image generation using textual inversion. arXiv preprint arXiv:2208.01618 (2022)
11. Hertz, A., Aberman, K., Cohen-Or, D.: Delta denoising score. In: Proceedings of the IEEE/CVF International Conference on Computer Vision. pp. 2328–2337 (2023)
12. Hertz, A., Mokady, R., Tenenbaum, J., Aberman, K., Pritch, Y., Cohen-Or, D.: Prompt-to-prompt image editing with cross attention control. arXiv preprint arXiv:2208.01626 (2022)
13. Ho, J., Jain, A., Abbeel, P.: Denoising diffusion probabilistic models. Advances in neural information processing systems **33**, 6840–6851 (2020)
14. Ho, J., Saharia, C., Chan, W., Fleet, D.J., Norouzi, M., Salimans, T.: Cascaded diffusion models for high fidelity image generation. The Journal of Machine Learning Research **23**(1), 2249–2281 (2022)
15. Hu, E.J., Shen, Y., Wallis, P., Allen-Zhu, Z., Li, Y., Wang, S., Wang, L., Chen, W.: LoRA: Low-rank adaptation of large language models. In: International Conference on Learning Representations (2022), <https://openreview.net/forum?id=nZeVKeeFYf9>
16. Kawar, B., Zada, S., Lang, O., Tov, O., Chang, H., Dekel, T., Mosseri, I., Irani, M.: Imagic: Text-based real image editing with diffusion models. arXiv preprint arXiv:2210.09276 (2022)
17. Kim, G., Kwon, T., Ye, J.C.: Diffusionclip: Text-guided diffusion models for robust image manipulation. In: Proceedings of the IEEE/CVF Conference on Computer Vision and Pattern Recognition. pp. 2426–2435 (2022)

18. Kwon, M., Jeong, J., Uh, Y.: Diffusion models already have a semantic latent space. arXiv preprint arXiv:2210.10960 (2022)
19. Luo, S., Tan, Y., Huang, L., Li, J., Zhao, H.: Latent consistency models: Synthesizing high-resolution images with few-step inference. arXiv preprint arXiv:2310.04378 (2023)
20. Meng, C., He, Y., Song, Y., Song, J., Wu, J., Zhu, J.Y., Ermon, S.: Sdedit: Guided image synthesis and editing with stochastic differential equations. arXiv preprint arXiv:2108.01073 (2021)
21. Mokady, R., Hertz, A., Aberman, K., Pritch, Y., Cohen-Or, D.: Null-text inversion for editing real images using guided diffusion models. In: Proceedings of the IEEE/CVF Conference on Computer Vision and Pattern Recognition. pp. 6038–6047 (2023)
22. Pan, Z., Gherardi, R., Xie, X., Huang, S.: Effective real image editing with accelerated iterative diffusion inversion. In: Proceedings of the IEEE/CVF International Conference on Computer Vision. pp. 15912–15921 (2023)
23. Peebles, W., Xie, S.: Scalable diffusion models with transformers. In: Proceedings of the IEEE/CVF International Conference on Computer Vision. pp. 4195–4205 (2023)
24. Pernias, P., Rampas, D., Aubreville, M.: Wuerstchen: Efficient pretraining of text-to-image models. arXiv preprint arXiv:2306.00637 (2023)
25. Podell, D., English, Z., Lacey, K., Blattmann, A., Dockhorn, T., Müller, J., Penna, J., Rombach, R.: Sdxl: Improving latent diffusion models for high-resolution image synthesis. arXiv preprint arXiv:2307.01952 (2023)
26. Radford, A., Kim, J.W., Hallacy, C., Ramesh, A., Goh, G., Agarwal, S., Sastry, G., Askell, A., Mishkin, P., Clark, J., Krueger, G., Sutskever, I.: Learning transferable visual models from natural language supervision. In: Meila, M., Zhang, T. (eds.) Proceedings of the 38th International Conference on Machine Learning. Proceedings of Machine Learning Research, vol. 139, pp. 8748–8763. PMLR (18–24 Jul 2021), <https://proceedings.mlr.press/v139/radford21a.html>
27. Ramesh, A., Dhariwal, P., Nichol, A., Chu, C., Chen, M.: Hierarchical text-conditional image generation with clip latents (2022)
28. Rombach, R., Blattmann, A., Lorenz, D., Esser, P., Ommer, B.: High-resolution image synthesis with latent diffusion models. In: Proceedings of the IEEE/CVF conference on computer vision and pattern recognition. pp. 10684–10695 (2022)
29. Rombach, R., Blattmann, A., Lorenz, D., Esser, P., Ommer, B.: High-resolution image synthesis with latent diffusion models (2022)
30. Ruiz, N., Li, Y., Jampani, V., Pritch, Y., Rubinstein, M., Aberman, K.: Dreambooth: Fine tuning text-to-image diffusion models for subject-driven generation. In: Proceedings of the IEEE/CVF Conference on Computer Vision and Pattern Recognition. pp. 22500–22510 (2023)
31. Saharia, C., Chan, W., Saxena, S., Li, L., Whang, J., Denton, E., Ghasemipour, S.K.S., Ayan, B.K., Mahdavi, S.S., Lopes, R.G., Salimans, T., Ho, J., Fleet, D.J., Norouzi, M.: Photorealistic text-to-image diffusion models with deep language understanding (2022)
32. Song, J., Meng, C., Ermon, S.: Denoising diffusion implicit models. In: 9th International Conference on Learning Representations, ICLR 2021, Virtual Event, Austria, May 3-7, 2021. OpenReview.net (2021), <https://openreview.net/forum?id=St1giarCHLP>
33. Wallace, B., Gokul, A., Naik, N.: Edict: Exact diffusion inversion via coupled transformations. In: Proceedings of the IEEE/CVF Conference on Computer Vision and Pattern Recognition. pp. 22532–22541 (2023)

34. Wang, Z., Jiang, Y., Zheng, H., Wang, P., He, P., Wang, Z., Chen, W., Zhou, M.: Patch diffusion: Faster and more data-efficient training of diffusion models. arXiv preprint arXiv:2304.12526 (2023)
35. Wu, C.H., De la Torre, F.: A latent space of stochastic diffusion models for zero-shot image editing and guidance. In: Proceedings of the IEEE/CVF International Conference on Computer Vision. pp. 7378–7387 (2023)
36. Yu, J., Wang, Y., Zhao, C., Ghanem, B., Zhang, J.: Freedom: Training-free energy-guided conditional diffusion model. arXiv preprint arXiv:2303.09833 (2023)
37. Zhang, L., Rao, A., Agrawala, M.: Adding conditional control to text-to-image diffusion models. In: Proceedings of the IEEE/CVF International Conference on Computer Vision. pp. 3836–3847 (2023)
38. Zhang, R., Isola, P., Efros, A.A., Shechtman, E., Wang, O.: The unreasonable effectiveness of deep features as a perceptual metric (2018)
39. Zhang, Z., Han, L., Ghosh, A., Metaxas, D.N., Ren, J.: Sine: Single image editing with text-to-image diffusion models. In: Proceedings of the IEEE/CVF Conference on Computer Vision and Pattern Recognition. pp. 6027–6037 (2023)
40. Zheng, H., He, P., Chen, W., Zhou, M.: Truncated diffusion probabilistic models and diffusion-based adversarial auto-encoders. arXiv preprint arXiv:2202.09671 (2022)

A Supplementary materials

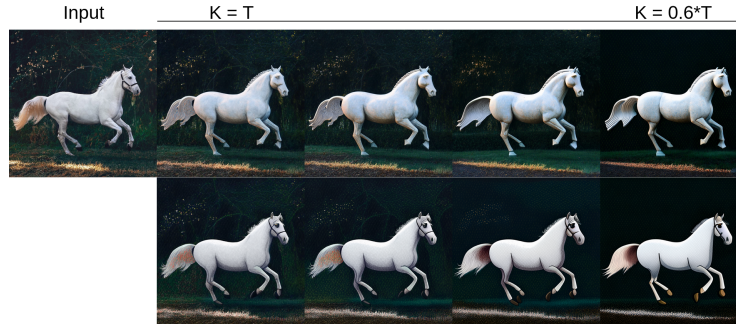


Fig. 11: Results with Wuerstchen. The images are 1024×1024 and each editing result is obtained in around 3 seconds. K controls the interval of alignment. Shorter alignment intervals lead to increased editing strength but less identity preservation. The edits are sculpture and cartoon

A.1 LASPA for videos and mobile diffusion

Our method has a strong advantage over prior methods in terms of speed. This renders our method more suitable for processing many frames and for results on mobile devices.

We show several clips on the webpage to showcase the performance on videos. We convert the input clips to frames, and we process each frame using our method. Even without the temporal information, our method shows promising results for future work. We test several realistic edits such as object replacement, as well as artistic edits. By fixing the unrestricted random latent for all frames, some continuity is achieved as seen in the attached videos.

Additionally, we demonstrate how the speed can be further increased by using text-to-image diffusion models that are faster than stable diffusion. We use Wuerstchen [24] which can generate 1024×1024 images in 3 seconds by using smaller inner representations. While the Wuerstchen uses DDPM sampling, we can still edit using input alignment. We showcase our results with high resolution images using different choices of alignment interval end K in Figure 11.

A.2 LASPA for LCM models

Recently, Latent Consistency Models (LCMs) for image synthesis [19] achieved high quality generation with fewer steps than pretrained stable diffusion. We show how our method naturally extends to LCM models. We use prediction of x_0 alignment to produce the results in Figure 12. All results were produced using the same parameters.

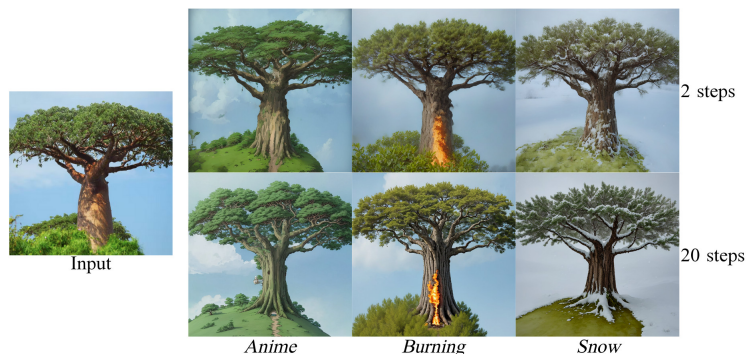


Fig. 12: LASPA can edit using LCMs in as few as two steps.

A.3 Facial editing with LASPA

As mentioned in the paper, accurate facial editing is possible with stricter parameters (lower scale, longer alignment interval, and higher interpolation coefficient). All the results in Figure 13 are produced with the same settings.

We can see that image preservation is very high. Letters in the background, accessories, and unique facial features are preserved with high accuracy. This is incredibly difficult to achieve with other generative models such as GANs.



Fig. 13: Facial editing results with our method. We observe that our method preserves details such as text on the clothing, accessories, and unique facial features.

A.4 Additional results

We present additional results to showcase our method.

Some animal swapping results from TEdBench show interesting results. The results are shown in Figure 14. We can see the quality of object replacement



Fig. 14: Extended results on TEDBench samples.

edits, even when changes to the outline of the object are required. In the middle row, we highlight the eagle example where different degrees of editing can be achieved. Eagle1 maintains the outline of the reference image exactly, leading to an eagle image that is more accurate but less realistic. Eagle2 shows a different possible result where the outline is not followed strictly, but the resulting image is more natural.

Additionally, we present additional results on a variety of images and edits in Figure 15.

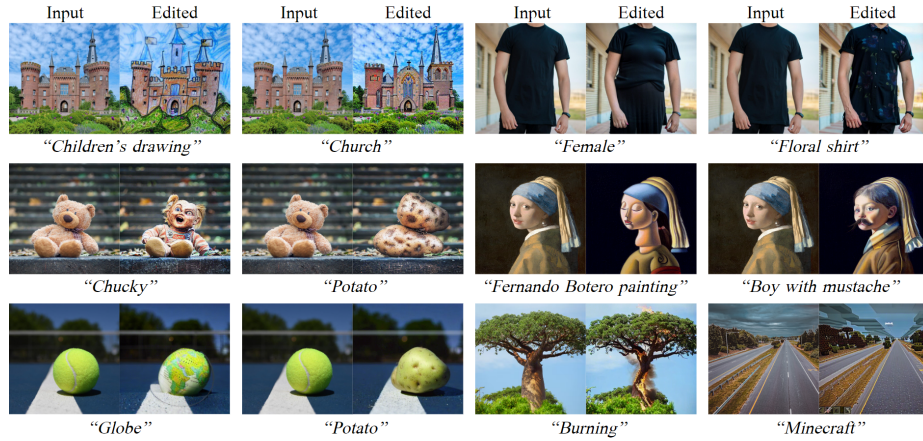


Fig. 15: Extended results on a variety of images and edits.

A.5 Additional visualizations of alignment

In the paper, we visualize the intermediate output when using input alignment (Figure 3, page 6). Here, we show results with $pred_{x_0}$ and ϵ_θ alignment. All of the results in Figure 16, were obtained with stable diffusion 2.1 on resolution 768×768 .

We can see that all three approaches lead to results that are faithful to both the input image and the prompt. Furthermore, the intermediate visualizations show that they are following a smooth and reasonable path of editing. Input alignment if applied in all steps (until $t=0$) leads to strong preservation of input image details. On the other hand, $pred_{x_0}$ alignment leads to stronger textual influence than input alignment. Error alignment while showing strong textual influence leads to lower image quality than input and $pred_{x_0}$ alignment.



Fig. 16: Extended visualization of our latent alignment. The editing prompt is “a photo of an angry woman”.

A.6 Additional comparisons against SINE

In Figure 17 we present additional results comparing LASPA to SINE. In most cases, SINE makes irrelevant changes to the shapes or colors of the reference image. LASPA, on the other hand, reflects the required textual edits with minimal changes to the input image. We believe that this is a direct result of using the spatial latent of the reference image to align. Shapes and colors of most irrelevant details are well preserved by LASPA. As we discuss in the following section, SINE finetunes an entire stable diffusion network with a modified prompt to preserve the input image. This proves to be problematic in some cases as reflected in their results.

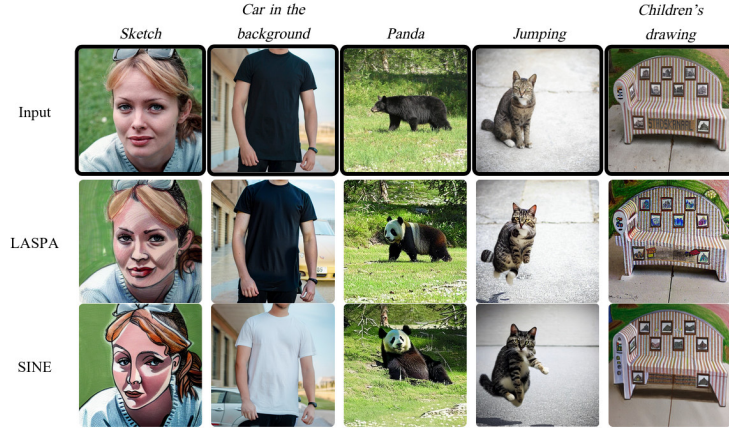


Fig. 17: SINE struggles to maintain some reference image details

A.7 Contrast with SINE

While Imagic optimizes a textual embedding as well as the network, SINE is more comparable to our method as it does not directly optimize the textual embedding. Instead, borrowing from previous works, SINE selects a special uncommon word (namely “sks”) and finetunes the network to reproduce the input image given the adjusted prompt. So given an image of a castle, SINE will finetune a stable diffusion network with the prompt “a photo of a sks castle”. The finetuned network serves only a single goal, which is reproducing the input image. That is the major difference between how SINE and our method preserve the input image.

The methods also differ in how edits are achieved. For SINE, two classifier-free guidance results are interpolated and they come from two different networks (the finetuned network and pretrained stable diffusion). In our case, we align latents of the pretrained network using *computed* reference latents.

Nonetheless, there are several shared ideas. Similar to our method, pretrained stable diffusion is utilized in SINE without modification as the source of word influence. Finetuning is required per image, but editing on the same image can be done at inference time with the same finetuned network. In addition, K and v in SINE achieve very similar effects to LASPA’s K and β . In a sense, SINE does latent alignment as well, albeit using a network finetuned with a special textual token. In general, SINE and LASPA share strengths and pitfalls. Both are significantly more faithful to the input image than Imagic. On the other hand, they both suffer from low quality results on large pose changes or with certain seeds.

However, with regards to performance LAPSAs is significantly faster and less complex to run. SINE requires 15 minutes of finetuning per image, storing a model per image, and running two models simultaneously at inference time. For datasets like TEDBench, the total size of the models is hundreds of Gigabytes

and the total time is several hours. LASPA, on the other hand, does not require storing additional models besides the pretrained stable diffusion and can perform any edit in 6 seconds.